JOURNAL OF GUIDANCE, CONTROL, AND DYNAMICS
Vol. 31, No. 3, May–June 2008

Decomposition-Based Simultaneous Stabilization with Optimal Control

Ruben E. Perez* and Hugh H. T. Liu†
University of Toronto, Toronto, Ontario M3H 5T6, Canada
and
Kamran Behdinan‡
Ryerson University, Toronto, Ontario M5B 2K3, Canada

DOI: 10.2514/1.31407

Simultaneous stabilization addresses the stability of multiple plants under a single feedback controller. It is desired for aircraft flight control operating under different conditions, when they are represented by a collection of linear dynamic models. The single controller brings continuity and a level of reliability. This paper presents a decomposition approach for the solution to the simultaneous stabilization problem. A bilevel design optimization architecture is adopted in which design of each individual plant (flight condition) is taking place at the bottom level, and the top-level optimization aims for single-control convergence of those individual controllers. Furthermore, performance requirements can be taken into account concurrently with the stabilization process, thanks to the separate bilevel decomposition concept. The effectiveness of the proposed approach is illustrated by different aircraft control system design test cases.

Nomenclature

A	=	state matrix
a_n	=	normal acceleration, g
B	=	input matrix
C	=	output matrix
$\mathbb{E}$	=	expected value
f	=	objective function
G	=	compatibility constraint
J	=	performance index
K	=	feedback control gain
p	=	roll rate, rad/s
q	=	pitch rate, rad/s
r	=	yaw rate, rad/s
T_e	=	elevator time constant, s
t	=	time, s
u	=	control vector
w	=	vertical velocity, ft/s
x	=	state vector
$\bar{x}$	=	local design variable
y	=	output vector
$\bar{y}$	=	coupling design variable
$\bar{z}$	=	global design variable
β	=	sideslip, rad
Δu	=	aircraft velocity, ft/s
$\Delta\theta$	=	pitch angle, rad
δ	=	deflection, rad
λ	=	eigenvalue
ϕ	=	roll angle, rad
ω	=	weighting factor

Subscripts

a	=	aileron
e	=	elevator
j	=	jth plant
r	=	rudder
SL	=	system level

Presented as Paper 6357 at the AIAA Guidance, Navigation, and Control Conference and Exhibit, Keystone, CO, 21–24 August 2006; received 3 April 2007; revision received 27 August 2007; accepted for publication 25 September 2007.

*Postdoctoral Research Associate, Institute for Aerospace Studies. Student Member AIAA
†Associate Professor, Institute for Aerospace Studies. Member AIAA.
‡Associate Professor and Chair, Department of Aerospace Engineering. Member AIAA

I. Introduction

SIMULTANEOUS stabilization (SS) addresses the stability of a finite collection of distinct plants under a single feedback controller. It is of interest for flight control applications in which an aircraft operating under different conditions is represented by a collection of flight dynamic models. A single stabilizing control provides system simplicity and reliability and can bring benefits to different types of aircraft. For example, it could be used as a backup control system under primary flight control systems failure situations for a commercial airplane or as an inexpensive control system alternative for small general aviation aircraft. In addition, it can be used as a backup reconfigurable control under actuation system damage or failure.

The simultaneous stabilization problem was first introduced by Saeks and Murray [1], based on the work of Birdwell et al. [2]. In the case of two plants, the simultaneous stabilization problem reduces to a well-known strong stabilization problem [3], in which a proper stable controller is found to stabilize both plants. However, simultaneous stabilization of more than two plants is, in general, undecidable, as demonstrated by Blondel and Gevers [4]. An analytical solution to the simultaneous stabilization problem is very difficult to find, due to the problem's nondeterministic polynomial-time (NP)-hard nature [5,6], and so no analytical algorithm can be devised to lead to a simple or rapid solution, and only an exhaustive analysis of all possible outcomes will lead to the solution. Finding a solution to the problem had relied instead on a variety of numerical approaches. Such approaches had focus in two main areas. The first deals with the solution to the simultaneous stabilization problem itself, in which the solution to the problem has been tackled from a number of different directions, including polynomial [7–9], minimum phase [10], pole placement [11], system inversion [12], and optimization-based [13–15] approaches, respectively. The second deals with performance improvement for the simultaneous stabilization, or simultaneous optimal control, in which nonlinear optimization algorithms have been proposed [16–19].

This paper presents a decomposition strategy for solving the simultaneous stabilization problem and improving its performance using a multidisciplinary design optimization analogy. Taking advantage of control effort decomposition, a feasible stabilizing controller with closed-loop stability for each individual plant can be found. Furthermore, the strategy is extended to deal with both simultaneous stabilization and performance improvement. The solution approach is applied to three different control-design case studies. The first deals with the stabilization of an aircraft longitudinal control system. The second deals with both stabilization and optimal tracking for an aircraft's longitudinal control system. The final example shows the application of simultaneous stabilization as an alternative for passive fault-tolerant control, in which optimal stabilization and tracking of an aircraft's lateral control system is performed for nominal and failure plants.

II. Simultaneous Stabilization Problem

A. Problem Formulation

Consider a set of N different proper plants described by the state-space equations:

$$\dot{x}_j(t) = A_j x_j(t) + B_j u_j(t), \qquad y_j(t) = C_j x_j(t) \tag{1}$$

where $x_j \in \Re^n$ and $u_j \in \Re^m$, for all $j \in I_N \triangleq \{1, \ldots, N\}$, where N is the number of plants.

The goal is to simultaneously stabilize each of the preceding systems by designing a single feedback compensator. To be more precise, we are looking for a feedback control law as

$$u_j(t) = -K y_j(t) \tag{2}$$

such that each system (1) with the feedback law is internally stabilizing. The closed-loop system is given then by

$$\dot{x}_j(t) = (A_j - B_j K C_j) x_j(t) \tag{3}$$

B. Simultaneous Stabilization Solution: Necessary and Sufficient Condition

Internal stabilization of the feedback law is equivalent to assuring that all eigenvalues of each closed-loop system have negative real parts. Therefore, there exists a solution to the simultaneous stabilization problem if and only if

$$\min_K I = \max_{1 \le i \le m, 1 \le j \le N} Re(\lambda_{i,j}) < 0 \tag{4}$$

where $\lambda_{i,j}$ is the ith eigenvalue of the jth closed-loop system given by Eq. (3). Inequality (4) represents the necessary and sufficient condition for the solvability of the simultaneous stabilization problem, because a solution to the problem will exist if and only if a control gain K, which minimizes the objective function I and makes it negative, can be found [14]. An equivalent formulation in which the objective function is continuously differentiable can be formulated as

$$\min_{K,\gamma} I = \gamma \quad \text{subject to} \quad Re(\lambda_{i,j}) \le \gamma \qquad i = 1, \ldots, m, \qquad j = 1, \ldots, N \tag{5}$$

C. Simultaneous Optimal Control

It is desired to design a controller that, in addition to the stabilization of a set of plants as formulated in Eq. (1), will provide good performance. The problem then becomes to design a feedback law as formulated in Eq. (2), which minimizes the plants' performance measures. In simultaneous stabilization, such measures have been defined based on a quadratic performance index [16] or as the upper bound of it, as [17–19]

$$\bar{J}_j = \mathbb{E}\left[\int_0^{t_f} [x_j^T(t) Q_i x_j(t) + u_j^T(t) R_j u_j(t)]\, \mathrm{d}t\right] \qquad j = 1, \ldots, N \tag{6}$$

each associated with one of the plants described in Eq. (1).

Standard linear-quadratic (LQ) assumptions are made for each system: namely, all members of collection $\{Q_j\}_{j \in I_n}$ are positive semidefinite and all members of $\{R_j\}_{j \in I_n}$ are strictly positive definite [20]. Furthermore, each system (A_j, B_j) is controllable and (A_j, C_j) is observable. The expectation operator $\mathbb{E}$ is taken over randomized initial conditions with zero mean ($\mathbb{E}\{x_0\} = 0$) and a covariance equal to the identity ($\mathbb{E}\{x_0 x_0^T\} = I$). The performance measures in Eq. (6) can be then expressed as [21]

$$\bar{J}_j = \mathrm{tr}\{P_j\} \tag{7}$$

where each $P_j > 0$ satisfies, for a given K, the Lyapunov equation:

$$P_j(A_j - B_j K C_j) + (A_j - B_j K C_j)^T P_j + (K C_j)^T R_j (K C_j) + Q_j = 0 \tag{8}$$

III. Decomposition Strategy for Simultaneous Stabilization

A. Decomposition Formulation

An analogy between the simultaneous stabilization problem and the general multidisciplinary design optimization (MDO) problem formulation can be established by realizing that each plant-stabilization process is equivalent to a discipline in the general MDO process shown in Fig. 1, in which the common design variable among all disciplines is the simultaneous stabilization control gain K, as shown in Fig. 1.

A bilevel optimization strategy that enables decoupling and decomposition is used to solve the simultaneous stabilization problem. It has its origins in multidisciplinary design optimization theory, at the system level (SL), the objective function is stated as

$$\min_{\bar{z}_{\mathrm{SL}}, \bar{y}_{\mathrm{SL}}} f(\bar{z}_{\mathrm{SL}}, \bar{y}_{\mathrm{SL}})$$
$$\text{subject to } G_j[\bar{z}_{\mathrm{SL}}, \bar{z}_j^*, \bar{y}_{\mathrm{SL}}, \bar{y}_j^*(\bar{x}_j^*, \bar{y}_k^*, \bar{z}_j^*)] = 0$$
$$j, k = 1, \ldots, n \qquad k \ne j \tag{9}$$

where f represents the system-level objective function, and G_j represents the compatibility constraints, one for each subsystem (n subsystems in total). Variables shared by all subsystems are defined as global variables $\bar{z}$. Variables calculated by a subsystem and required by another subsystem are defined as coupling variables $\bar{y}$. Variables with a superscript asterisk indicate optimal values for the subsystem optimization, where $\bar{z}_j^*$, $\bar{y}_j^*$, and $\bar{x}_j^*$ are the jth subsystem optimal global, coupling, and local variables, respectively. Note that the system-level constraint assures simultaneous coordination of the coupled disciplinary values.

The lower subsystem-level (SSL) objective function is formulated such that it minimizes the discrepancy between the given system-level variables and the subsystem variables that meet the local disciplinary constraints. At the disciplinary level, the jth subsystem optimization is stated as

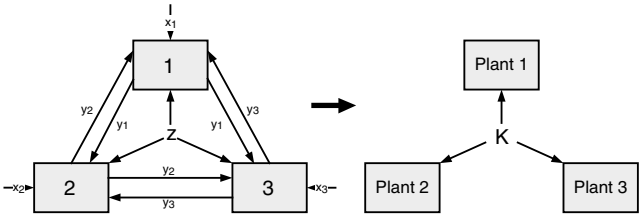

Fig. 1 Multidisciplinary optimization problem and simultaneous stabilization problem.

$$\min_{\bar{z}_j,\bar{y}_j,\bar{x}_j} G_j[\bar{z}_{\mathrm{SL}}, \bar{z}_j, \bar{y}_{\mathrm{SL}}, \bar{y}_j(\bar{x}_j, \bar{y}_k, \bar{z}_j)]$$
$$= \sum(\bar{z}_{\mathrm{SL}} - \bar{z}_j)^2 + \sum(\bar{y}_{\mathrm{SL}} - \bar{y}_j)^2 \quad (10)$$
$$\text{subject to } g_j[\bar{x}_j, \bar{z}_j, \bar{y}_j(\bar{x}_j, \bar{y}_k, \bar{z}_j)] \le 0$$

where $\bar{x}$ are local disciplinary design variables, and g are the specific disciplinary constraints.

B. Decomposed Equivalent of Necessary and Sufficient Conditions

In a simultaneous stabilization process, each plant-stabilization effort will be decomposed at the subsystem level, and the system level will ensure stabilization with a unique control gain K. Using the preceding formulation, a decomposed equivalent of Eq. (4) can be formulated as

$$\mathrm{SL}\,|\min_{K_{\mathrm{SL}},\gamma_{\mathrm{SL}}} I = \gamma_{\mathrm{SL}} \quad \text{subject to } G_j^* = 0 \qquad j = 1,\ldots,n$$
$$\mathrm{SSL}_j|\min_{K_j,\gamma_j} G_j = (K_j - K_{\mathrm{SL}})^2 + (\gamma_j - \gamma_{\mathrm{SL}})^2 \quad \text{subject to } Re(\lambda_{i,j}) \le \gamma_j$$
$$i = 1,\ldots,m \quad (11)$$

where both system- and subsystem-level objective functions are continuously differentiable. As in Eq. (5), a solution to the simultaneous stabilization problem will exist if and only if the system level converges with an optimal control gain K, which minimizes the system-level objective function I and makes it negative. Furthermore, at convergence, the subsystems compatibility constraints are met ($G_j = 0$), which implies that for each subsystem, $K_j = K_{\mathrm{SL}}$ and $\gamma_j = \gamma_{\mathrm{SL}}$; thus, each plant is stabilized by the optimum gain and $Re(\lambda_{i,j}) \le \gamma_{\mathrm{SL}}$, and so the formulation reduces to Eq. (5).

C. Decomposed Simultaneous Optimal Control

The equivalent decomposition strategy presented in Eq. (11) can be adapted further to achieve the simultaneous stabilization of plants while providing optimal performance as

$$\mathrm{SL}\,|\min_{K_{\mathrm{SL}}} I = \sum_{j=1}^{N} \omega_j J_j^*(K_j^*) \quad \text{subject to } G_j^* = 0 \qquad j = 1,\ldots,N$$
$$\mathrm{SSL}_j|\min_{K} G_j = (K - K_{\mathrm{SL}})^2 \quad \text{subject to } \begin{cases} Re(\lambda_{i,j}) \le \gamma' & i = 1,\ldots,m \\ g_j \le 0 \end{cases} \quad (12)$$

where J_j^* is a specified performance measure evaluated for each plant with the found subsystem-level optimal gain K_j^*, and $\omega_{j=1,\ldots,N}$ are suitable positive weighting factors.

Note that the simultaneous stabilization and optimal performance are addressed by the proposed formulation. The system-level optimization process will minimize the performance measure for each controller, while enforcing a unique gain solution for all plants with the system-level constraint. The subsystem optimization process will ensure internal stabilization of the feedback control law by using the specified stability boundary value γ' and enforce other desired dynamic characteristics using g_j constraints, while minimizing the discrepancy with the proposed system-level gain solution.

Depending on the stabilization problem, the preceding formulation can solve the simultaneous optimal control or stochastic simultaneous optimal control formulations, by specifying an adequate performance index. In the first case, the performance index is given directly from

$$J_j^* = \int_0^{t_f} \frac{1}{2}[x_j^T Q_j x_j + u_j^T R_j u_j]\,\mathrm{d}t$$

requiring a direct numerical evaluation of the integral for the given subsystem optimal gains. In the second case, the performance measure is evaluated from Eq. (8), where P_j satisfies the Lyapunov equation (9) for the obtained subsystem-level optimal gain.

IV. Test Cases

Three illustrative cases are implemented to demonstrate the effectiveness of the proposed simultaneous stabilization and simultaneous optimal control strategies. A sequential quadratic programming (SQP) optimization algorithm [22] was used at both the system and subsystem levels for the proposed strategies. Tolerance for the optimization procedure at both levels was defined on the order of 10^{-6}. Convergence of the optimization procedure is given when the search direction, maximum constraint violation, and first-order optimality measure is less than a specified tolerance.

A. Test Case 1

The first test case entails the simultaneous stabilization of the longitudinal dynamics short-period mode of an F4E fighter jet at four different operating points. It was proposed originally by Ackermann [23] and has been used as a benchmark problem by a number of other relevant references [13,14,17]. The system is described in linear time-invariant state-space form for all conditions as

$$\dot{x}_j(t) = A_j x_j(t) + B_j u_j, \qquad y_j(t) = C_j x_j(t) \qquad j = 1{:}4 \quad (13)$$

where the original longitudinal dynamics state-space vector component that includes normal acceleration and pitch rate has been extended to include the elevator actuator dynamics represented by a first-order low-pass filter, so that

$$x(t) = [a_n \;\; q \;\; \delta_e]^T \quad (14)$$

A stability-augmentation system characterized by a single static output feedback gain matrix K [Eq. (2)], with reference actuator command signal u_{com} representing the demanded deviation of the elevator deflection from its trim position, is used as

$$u_j(t) = u_{\mathrm{com}} - Ky_j(t) = u_{\mathrm{com}} - [k_{a_n} \;\; k_q \;\; k_{\delta_e}]C_j x_j(t) \quad (15)$$

The four flight operating conditions are significantly distinct from each other, with variation in both altitude and speed, as shown in Table 1. The plant-state coefficient matrices, control coefficient vectors, and output matrices are given as

$$A_j = \begin{bmatrix} a_{11_j} & a_{12_j} & a_{13_j} \\ a_{21_j} & a_{22_j} & a_{23_j} \\ 0 & 0 & -30 \end{bmatrix}, \qquad B_j = \begin{bmatrix} b_{1_j} \\ 0 \\ 30 \end{bmatrix}, \qquad C_j = \mathrm{I} \quad (16)$$

where the values of the matrices' parameters are given in Table 1.

It should be noted that the open-loop system is unstable at operating points 1 to 3, as can be seen from Table 2.

1. *Decomposed Equivalent Result*

Results of the simultaneous stabilization necessary and sufficient conditions problem formulation (5) obtained by Howitt and Luus [14] and compared with the proposed decomposed equivalent (11) are presented in Table 3. It can be seen from the table that the

Table 1 Flight operating conditions

Operating point	1	2	3	4
Mach number	0.5	0.9	0.85	1.5
Altitude, ft	5000	35,000	5000	35,000
a_{11}	−0.9896	−0.6607	−1.7202	−0.5162
a_{12}	17.41	18.11	50.72	26.96
a_{13}	96.15	84.34	263.5	178.9
a_{21}	0.2648	0.08201	0.2201	−0.6896
a_{22}	−0.8512	−0.6587	−1.418	−1.225
a_{23}	−11.89	−10.81	−31.99	−30.38
b_1	−97.78	−272.2	−85.09	−175.6

Table 2 Open-loop-system eigenvalues

Matrix	Eigenvalues
A_1	−30.0000, 1.2278, and −3.0686
A_2	−30.0000, 0.5590, and −1.8784
A_3	−30.0000, 1.7842, and −4.9042
A_4	−30.0000 and $-0.8706 \pm 4.2972i$

Table 3 Decomposed equivalent formulation comparison

	Howitt and Luus [14]	Decomposed equivalent
K^*	−0.10831	−0.114986
	−2.0000	−2.125059
	−1.1523	−1.171371
I^*	−1.88643	−1.88646

Table 4 Simultaneous optimal control performance indices comparison

	Proposed algorithm	HL [16]
J_1^*	1.5945	1.4140
J_2^*	1.5339	1.4866
J_3^*	1.5201	1.5192
J_4^*	1.5000	2.3410
I^*	6.1485	6.7609

proposed formulation led to results similar to those obtained by Howitt and Luus, in which the decomposed method yields a slightly better controller with a lower maximum eigenvalue.

2. Simultaneous Optimal Control Result

a. Optimal Control Results. The example is also applied for simultaneous optimal control, in which a linear-quadratic performance measure is used with a specified initial condition given by $x_0 = [1, 1, 1]^T$. As in [16,17], we set $R_j = 1$ and $Q_j = I$ for $j = 1, \ldots, 4$ for the performance measure. After 39 system-level iterations, an optimal gain vector K^* was obtained as

$$K^* = [-0.209582 \quad -1.373644 \quad 1.584912]$$

All pole locations for all plants lie in the negative real axis for the optimal gain found. Table 4 also shows the performance indices for such gain. A lower objective function value I is obtained by the proposed methodology, when compared with the performance indices found in [14]) for the same initial condition.

b. Stochastic Simultaneous Optimal Control Results. The simultaneous optimal control formulation in its stochastic form using Eq. (12) with the performance measure given by Eq. (6) is also used to solve the problem. Using this approach, after 92 system-level iterations, an optimal gain vector K^* was obtained as

$$K^* = [-1.096570 \quad -8.315312 \quad 4.296874]$$

Table 5 shows the values of each plant performance measure [trace (P_j)] resulting from solving the Lyapunov equation (8) for the optimal gain found by the proposed approach, as well as those performance measures obtained from other references. The minimal performance was obtained by our approach with $I = 31.48709$; however, such a result is similar to results obtained by other methods. Also note that our optimal solution leads to a lower guaranteed-cost bound when compared with other approaches, without directly specifying minimum bound constraints.

Table 6 shows the closed-loop-system eigenvalues using the stochastic optimal gain values. All pole locations for all plants are in the negative real axis. Hence, the optimal state-feedback gain found

Table 5 Stochastic optimal control performance indices comparison

	Proposed Algorithm	LC [19]	PSTM [17]	LDA [18]	HL [14]
J_1^*	2.50519	2.5046	2.5052	2.41	3.2494
J_2^*	9.62207	9.6217	9.6220	10.4	20.6696
J_3^*	14.06625	14.068	14.0662	15.3	12.9148
J_4^*	5.29359	5.2928	5.2936	5.22	7.6020
I^*	31.48709	31.4871	31.4871	33.33	44.4358

Table 6 Optimal gain closed-loop-system eigenvalues

Matrix	Eigenvalues
$A_1 - B_1KC_1$	−253.8746, −3.4369, and −10.6582
$A_2 - B_2KC_2$	−437.1375, −1.8523, and −19.7222
$A_3 - B_3KC_3$	−244.3152 and $-5.5091 \pm 12.8011i$
$A_4 - B_4KC_4$	−332.4771, −8.3368, and −12.3912

provides a control law that simultaneously stabilized the plants representing the four operating conditions for the F4E aircraft. To further illustrate this result, simulations of the resulting closed-loop systems are presented in Figs. 2–4. From these simulations, one can see that the closed-loop system is stable at each operating point. Furthermore, the obtained controller is, overall, stable in the interval between each analyzed operating point, as demonstrated from a Kharitonov [24] theorem analysis with polynomial manifolds defined from the extreme values between all the closed-loop-system characteristic equation polynomials.

B. Test Case 2

The second test case involves the design of a simultaneous stabilizing pitch-tracking control for a CRJ-200 regional jet aircraft at six significantly distinct flight operating conditions. The aircraft dynamics were extended to include actuator dynamics and are represented by the following system:

$$\underbrace{\begin{bmatrix} \dot{\Delta u} \\ \dot{w} \\ \dot{q} \\ \dot{\Delta\theta} \\ \dot{\delta}_e \end{bmatrix}}_{\dot{x}} = \underbrace{\begin{bmatrix} \hat{A}_j & \hat{B}_j \\ 0 & -\frac{1}{T_e} \end{bmatrix}}_{A} \underbrace{\begin{bmatrix} \Delta u \\ w \\ q \\ \Delta\theta \\ \delta \end{bmatrix}}_{x} + \underbrace{\begin{bmatrix} 0 \\ \frac{1}{T_e} \end{bmatrix}}_{B} \underbrace{\delta}_{\substack{c \\ u}} \tag{17}$$

where the elevator dynamics are represented as a first-order lag filter with a time constant T_e of 1.6 s.

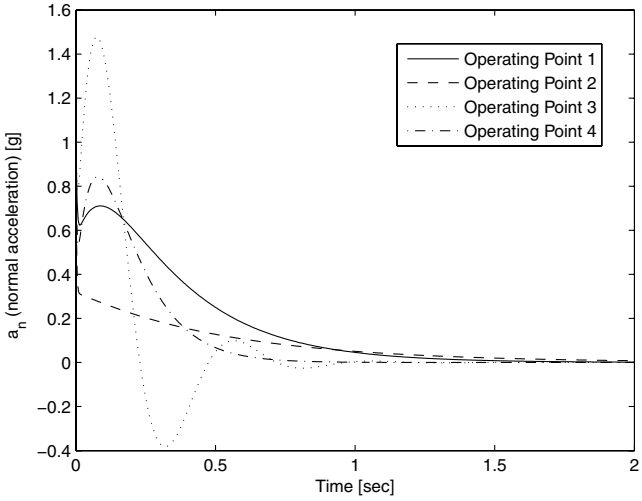

Fig. 2 Normal acceleration response; initial condition [1 0 0]′.

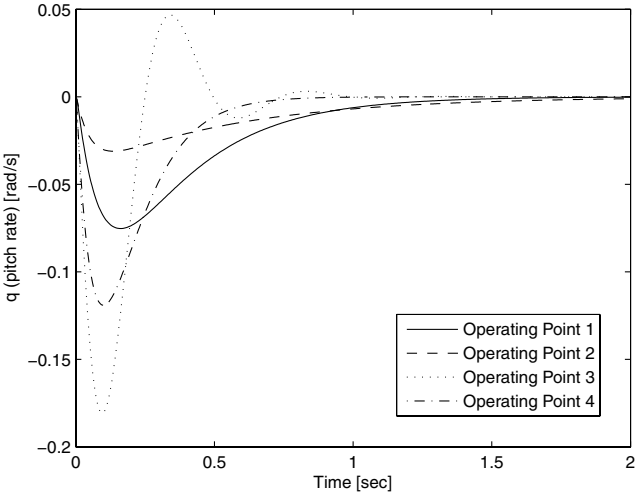

Fig. 3 Pitch rate response; initial condition [1 0 0]′.

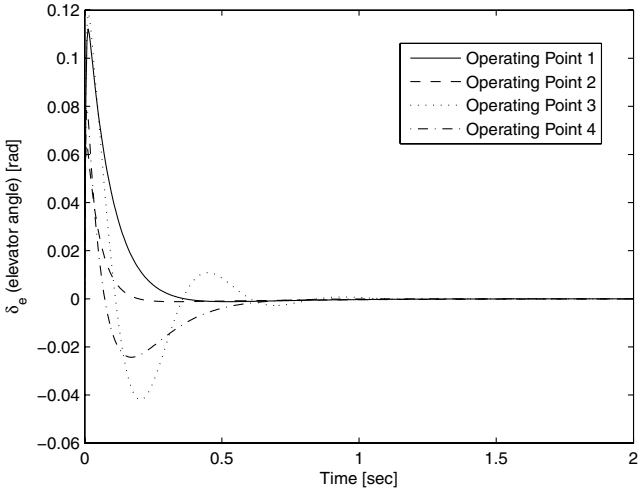

Fig. 4 Elevator deflection response; initial condition [1 0 0]′.

The operating flight conditions selected spans over the flight envelope, as shown in Table 7. The basic aircraft dynamics plant-state coefficient matrices and control coefficient vectors for each flight condition are given as

$$\hat{A}_j = \begin{bmatrix} a_{11_j} & a_{12_j} & 0 & a_{14_j} \\ a_{21_j} & a_{22_j} & a_{23_j} & a_{24_j} \\ a_{31_j} & a_{32_j} & a_{33_j} & a_{34_j} \\ 0 & 0 & 1 & 0 \end{bmatrix}, \qquad \hat{B}_j = \begin{bmatrix} 0 \\ b_{1_j} \\ b_{2_j} \\ 0 \end{bmatrix}, \qquad \hat{C}_j = \mathrm{I} \tag{18}$$

where the values of the matrices parameters are given in Table 7.

A LQ tracker for the pitch angle is used, as shown in Fig. 5. Note that one control input is available, and so exact tracking of one state is possible.

Define $C_z = [0\ 0\ 0\ 1\ 0]$ and extend the state vector x by the integral state x_I. Note that $\dot{x}_I = e$, where e is the tracking error. The extended system can be read from the following diagram:

$$\underbrace{\begin{bmatrix} \dot{x} \\ \dot{x}_I \end{bmatrix}}_{\dot{\bar{x}}} = \underbrace{\begin{bmatrix} A & 0 \\ -C_z & 0 \end{bmatrix}}_{\bar{A}} \underbrace{\begin{bmatrix} x \\ x_I \end{bmatrix}}_{\bar{x}} + \underbrace{\begin{bmatrix} B \\ 0 \end{bmatrix}}_{\bar{B}} u + \underbrace{\begin{bmatrix} 0 \\ 1 \end{bmatrix}}_{\bar{W}} \theta_c \tag{19}$$

$$u = -[K_x, K_I]\bar{x} = -\bar{K}\,\bar{x}$$

Table 8 presents the aircraft open-loop-system eigenvalues. It can be seen that the system is phugoid unstable at operating points 2 to 6.

The simultaneous optimal control formulation is used to solve the problem in its stochastic form using Eq. (12) with the performance measure given by Eq. (6). The state Q and control R weight-matrices terms are chosen using the maximum-allowable deviations of the states [25] so that $Q = \mathrm{diag}\{q_1, q_2, q_3, q_4, q_5\}$ and $R = \mathrm{diag}\{r_1\}$. For the Canadair Regional Jet (CRJ) pitch-tracking controller, the maximum-allowable state deviations are selected, as shown in Table 9. For the control effort, cost matrix $r_1 = 10^6$ was selected.

Using the proposed approach, after 51 system-level iterations, an optimal gain vector K^* was obtained as

$$K^* = [-0.000597\ \ 0.002211\ \ -0.337128$$
$$-1.678606\ \ 0.923064\ \ 0.651913]$$

Table 10 shows the closed-loop-system eigenvalues using the optimal pitch-tracker controller. It can be seen that all pole locations for all plants are in the negative real axis.

Table 7 CRJ-200 reference flight conditions

	Flight condition					
Property	1	2	3	4	5	6
Total weight	40,000	40,000	40,000	40,000	40,000	40,000
x position of c.g. x_{cg}, ft	$0.16\bar{c}$	$0.16\bar{c}$	$0.16\bar{c}$	$0.16\bar{c}$	$0.16\bar{c}$	$0.16\bar{c}$
Moment of inertia I_x slug · ft^2	55,717	55,717	55,717	55,717	55,717	55,717
Moment of inertia I_y, slug · ft^2	369,830	369,830	369,830	369,830	369,830	369,830
Moment of inertia slug · ft^2	411,017	411,017	411,017	411,017	411,017	411,017
Moment of inertia I_{xz} slug · ft^2	17,789	17,789	17,789	17,789	17,789	17,789
Mach number	0.74	0.55	0.48	0.42	0.37	0.28
Altitude, ft	33,000	33,000	19,000	19,000	5000	5000
Angle of attack, deg	0.7	0.7	0.7	0.7	0.7	0.7
Flight path angle, deg	0	0	0	0	0	0
a_{11}	−0.0084	−0.0002	−0.0001	−0.00001	0.00001	0.0001
a_{12}	0.0066	0.0146	0.0171	0.0206	0.023	0.0318
a_{14}	−32.198	−32.198	−32.198	−32.198	−32.198	−32.198
a_{21}	−0.1221	−0.1375	−0.1425	−0.1584	−0.1671	−0.2149
a_{22}	−0.8338	−0.5586	−0.8251	−0.7095	−1.0116	−0.7545
a_{23}	718.744	533.551	489.778	428.541	393.3341	297.673
a_{24}	−0.3935	−0.3927	−0.3921	−0.3919	−0.391	−0.3909
a_{31}	0.0001	0.0001	0.0001	0.0001	0.0001	0.0001
a_{32}	−0.0135	−0.0095	−0.0142	−0.0123	−0.0174	−0.0130
a_{33}	−0.6610	−0.4397	−0.6490	−0.5564	−0.7932	−0.5882
a_{34}	0.0001	0.0001	0.0001	0.0001	0.0002	0.0002
b_2	−52.179	−26.656	−36.754	−36.884	−36.884	−20.8087
b_3	−7.0588	−3.6180	−4.9911	−5.0157	−5.0157	−2.8311

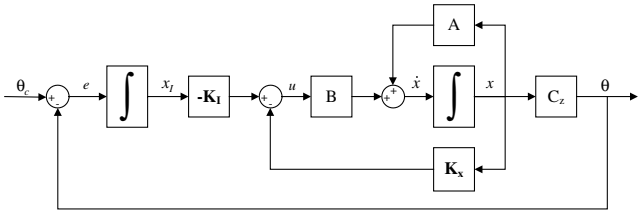

Fig. 5 LQ tracker for pitch angle.

To experimentally demonstrate the effectiveness of the simultaneous stabilization approach, the pitch-tracking control was verified to achieve the expectation, with the help of our integrated system design and flight simulation platform [26]. It consists of a state-of-the-art flight-training-device research simulator that is interconnected either with a real-time systems simulator or with Matlab/Simulink in a computer terminal, as shown in Fig. 6. Currently, the platform is used for control system design, simulation, and testing. This experimental testbed setup presents a more complete and realistic aircraft model, which includes factors not taken into account in the control system development, providing a suitable proof-of-concept facility.

The pitch-tracker control performance from the testbed at all six operating conditions is shown in Figs. 7 and 8 for a step input of 5 deg for the pitch angle. Table 11 also shows the tracker time-response characteristics from the tested conditions. It can be seen that the controller found provides adequate pitch-tracking characteristics for all of the selected operating points.

C. Test Case 3

The third example considers the use of simultaneous stabilization as a robust alternative for passive fault-tolerant control. In a classical passive fault-tolerant control, compensators are found using control reconfiguration for each assumed failure, trying to match the performance of the nominal plant. The application of the proposed methodology avoids reconfiguration calculations and allows us to provide internal stabilization and an adequate level of performance, similar to the nominal plant using a single control. A large range of distinct variations of the plant dynamics due to the presence of failures can be considered, as long as a simultaneous stabilization solution is found [see Eq. (4)]. This can prove beneficial when there is a limited capability to detect, identify, and isolate failures. The control reconfiguration example formulated in [27] is considered, in which a nominal lateral dynamics of an F4E is used, as presented in Eq. (20):

$$\dot{x} = A_n x + B_n u \qquad y = C_n x$$

$$A_n = \begin{bmatrix} -1.768 & 0.415 & -14.25 & 0 \\ -0.0007 & -0.3831 & 6.038 & 0 \\ 0.0016 & -0.9975 & -0.1551 & 0.0586 \\ 1 & 0 & 0 & 0 \end{bmatrix} \tag{20}$$

$$B_n = \begin{bmatrix} 1.744 & 8.952 \\ -2.92 & -0.3075 \\ 0.0243 & -0.0036 \\ 0 & 0 \end{bmatrix} \qquad C_n = I$$

The state vector consists of roll rate p (rad/s), yaw rate r (rad/s), sideslip β (rad), and roll angle ϕ (rad) (i.e., $x = [p \;\; r \;\; \beta \;\; \phi]^T$). The control vector consists of rudder δ_r and aileron δ_a (i.e., $u = [\delta_r \;\; \delta_a]^T$).

The roll and sideslip angles are tracked while considering several deviations from the nominal plant due to failures; specifically, the simultaneous stabilization control is designed for the nominal plant and the following failures cases:

1. Failure 1

Aileron effectiveness is reduced by half; that is, the second column of B_n is multiplied by 0.5. This failure is equivalent to a loss of aileron surface area, which reduces the available rolling control moment.

2. Failure 2

The first row of A_n is reduced by half. This corresponds to an overall decrease in the aerodynamic forces that contribute to the roll, as might result from battle damage to the wings.

3. Failure 3

The third row of A_n is reduced by half. This corresponds to an overall decrease in the side-force aerodynamic forces.

4. Failure 4

The rudder coupling to roll rate is reduced by tenfold; i.e., the first row, first column of B_n is multiplied by 0.1.

5. Failure 5

The second row, second column of A_n is reduced by half, and the second row, third column of A_n is reduced by tenfold. This corresponds to a decrease in the airframe's yaw damping and directional stability, respectively.

A tracking control structure similar to that shown in Fig. 5 is used. The tracking problem is solved using the simultaneous optimal control formulation in its stochastic form [Eq. (12)] with the

Table 8 Open-loop-system eigenvalues

Matrix	Eigenvalues
A_1	$-0.7478 \pm 3.1074i$ and $-0.0037 \pm 0.0745i$
A_2	$-0.4999 \pm 2.2539i$ and $0.0007 \pm 0.0912i$
A_3	$-0.7380 \pm 2.6316i$ and $0.0009 \pm 0.0955i$
A_4	$-0.6343 \pm 2.2887i$ and $0.0013 \pm 0.1073i$
A_5	$-0.9040 \pm 2.6148i$ and $0.0016 \pm 0.1132i$
A_6	$-0.6745 \pm 1.9653i$ and $0.0032 \pm 0.1472i$

Table 9 State weight matrix maximum-allowable deviations

q_j value	Equally tolerable state derivation
$q_1 = 1/(16.4)^2$	Δu: 16.4 ft/s
$q_2 = 1/(3.28)^2$	w: 3.28 ft/s
$q_3 = 1/(1000 \times 0.0175)^2$	q: 1000 deg/s
$q_4 = 1/(5 \times 0.0175)^2$	θ: 5 deg
$q_5 = 1/(10 \times 0.0175)^2$	δ: 24 deg
$q_6 = 1/(0.1 \times 0.0175)^2$	x_I: 0.1 deg

Table 10 Pitch-tracker system closed-loop-system eigenvalues

Matrix	Eigenvalues
A_1–B_1KC_1	$-0.7816 \pm 3.2119i$, $-0.3426 \pm 0.5545i$, -0.0097, and -0.4470
A_2–B_2KC_2	$-0.4428 \pm 2.3058i$, $-0.2624 \pm 0.3134i$, -0.7857, and -0.0043
A_3–B_3KC_3	$-0.6648 \pm 2.7010i$, $-0.3169 \pm 0.4083i$, -0.0035, and -0.7092
A_4–B_4KC_4	$-0.5315 \pm 2.3420i$, $-0.2689 \pm 0.3494i$, -0.0052, and -0.8619
A_5–B_5KC_5	$-0.7879 \pm 2.6720i$, $-0.3329 \pm 0.4451i$, -0.0043, and -0.7607
A_6–B_6KC_6	$-0.5114 \pm 1.9982i$, $-0.2442 \pm 0.3564i$, -0.0096, and -1.0235

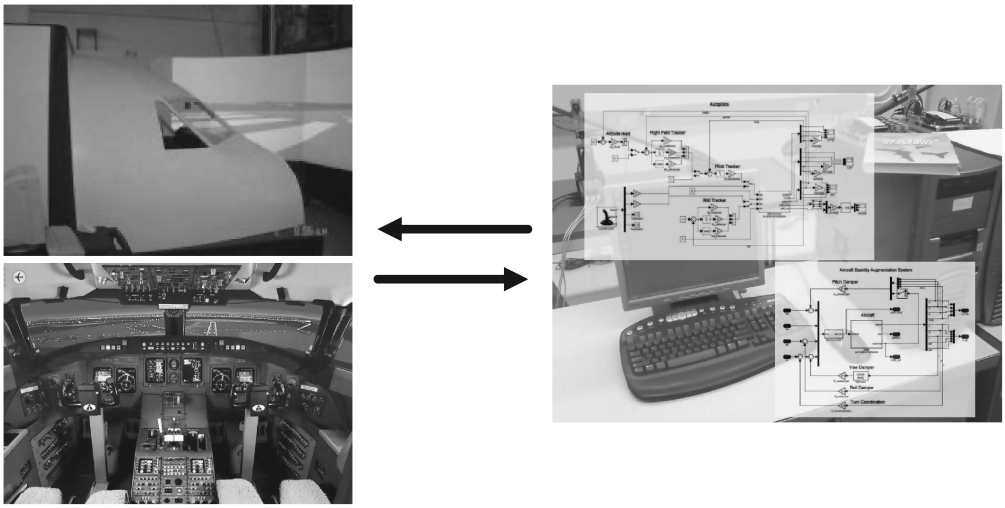

Fig. 6 Integrated control design and flight simulation platform.

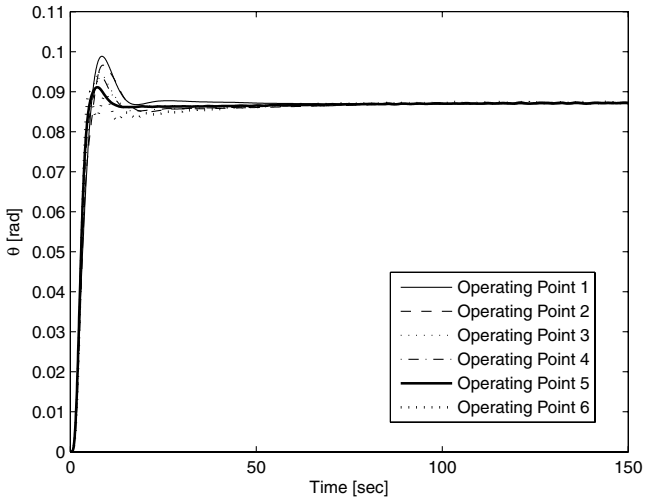

Fig. 7 Pitch-angle tracking for a 5-deg pitch-angle step input.

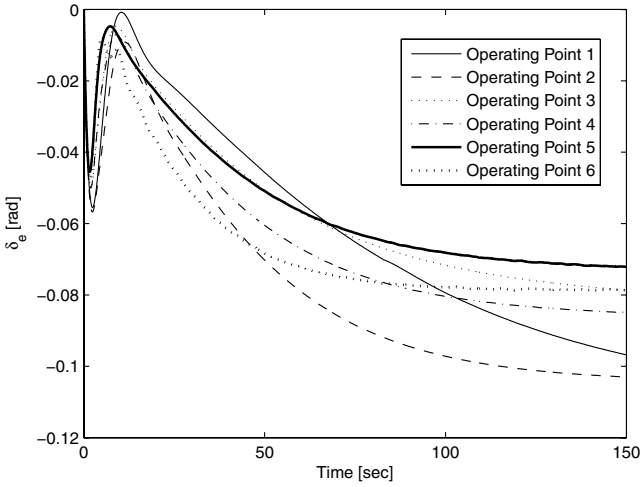

Fig. 8 Elevator deflection for a 5-deg pitch-angle step input.

performance measure given by Eq. (6). The state Q and control R weight-matrices terms are set for the performance measure as $R_1 = 0.1$, $R_2 = 0.1$, and $Q_j = I$ for $j = 1, \ldots, 6$. After 63 system-level iterations, an optimal gain vector K^* is obtained as

$$K^* = \begin{bmatrix} 0.283 & -2.411 & 3.176 & 0.516 & -2.844 & -0.224 \\ 2.847 & 0.455 & -1.828 & 5.000 & 0.467 & -2.851 \end{bmatrix}$$

As with the previous test cases, the closed-loop-system eigenvalues using the found optimal tracker controller are in the negative real axis. Figures 9 and 10 show the time histories of the plant states and control inputs for all the considered cases, when the aircraft is subject to a 10-deg roll angle and 5-deg sideslip tracking commands.

It can be seen that the controller found provides adequate pitch-tracking characteristics for the nominal and failure cases. Note how the state-response plots between the nominal plan and the failure cases are very close to each other, which implies that despite the severity of the failures, the control found is able to successfully recover the dynamics of the nominal model. The yaw- and roll-angle responses of the failed and nominal systems are almost indistinguishable for most of the cases, whereas the aileron exhibits higher activity with no significant change in rudder motion. When the aileron effectiveness was reduced in the first failure case, the system simply increased the aileron motions with no apparent change in rudder activity. This is because the rudder is an ineffective surface for roll control at this flight condition. Although a reconfigurable control system deals with each failure on a one-by-one basis [27], the simultaneous stabilization controller finds a unique control law that provides an adequate level of performance for the nominal case and for all the distinct failure cases.

Table 11 Pitch-tracker time-response characteristics

Flight condition	Rise time, s	Settling time, s	Overshoot, %	Steady-state error, %
1	3.2344	9.0805	5.9799	0.1092
2	3.6870	13.9664	10.647	0.1028
3	3.4520	11.6801	8.9070	0.0375
4	3.5538	13.0313	10.996	0.1834
5	3.3135	10.9605	8.7607	0.1171
6	3.4117	18.9931	12.710	0.5315

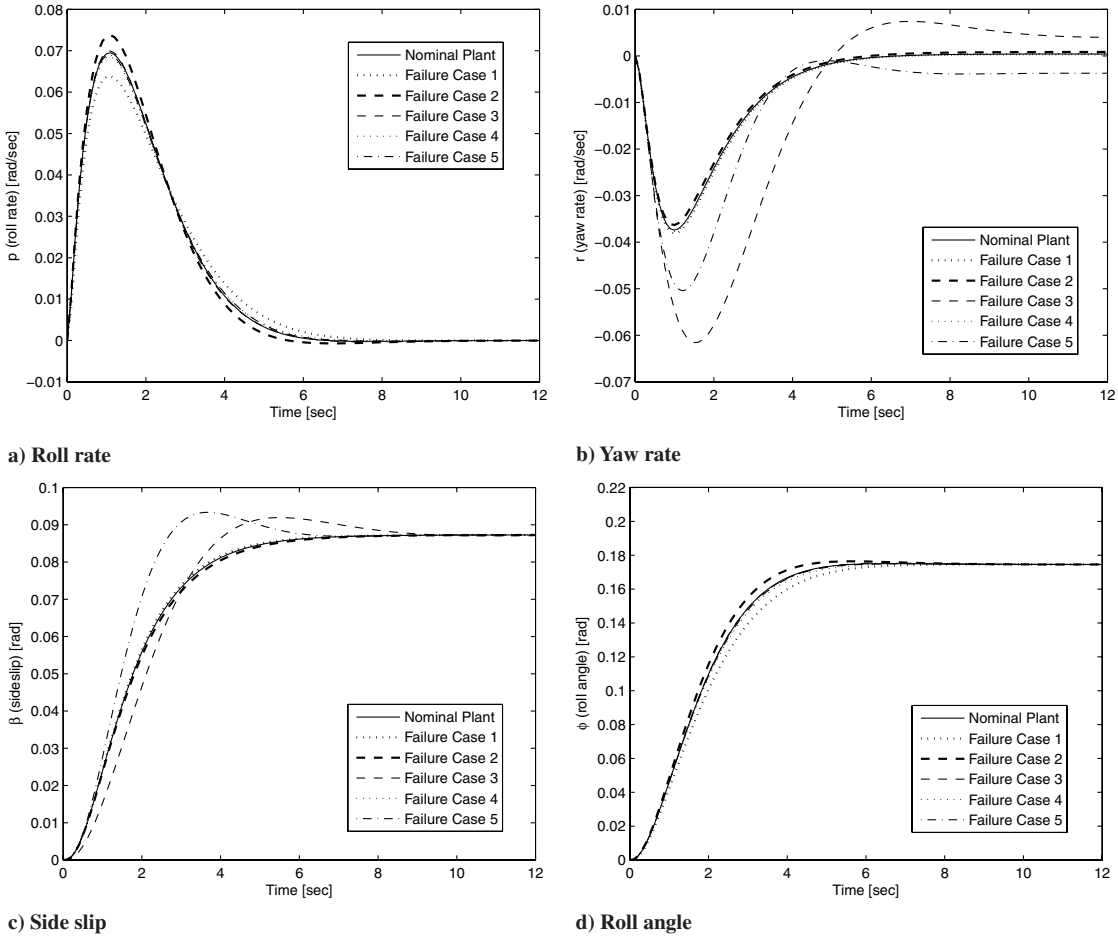

a) Roll rate **b) Yaw rate**

c) Side slip **d) Roll angle**

Fig. 9 F4E states responses to tracking commands.

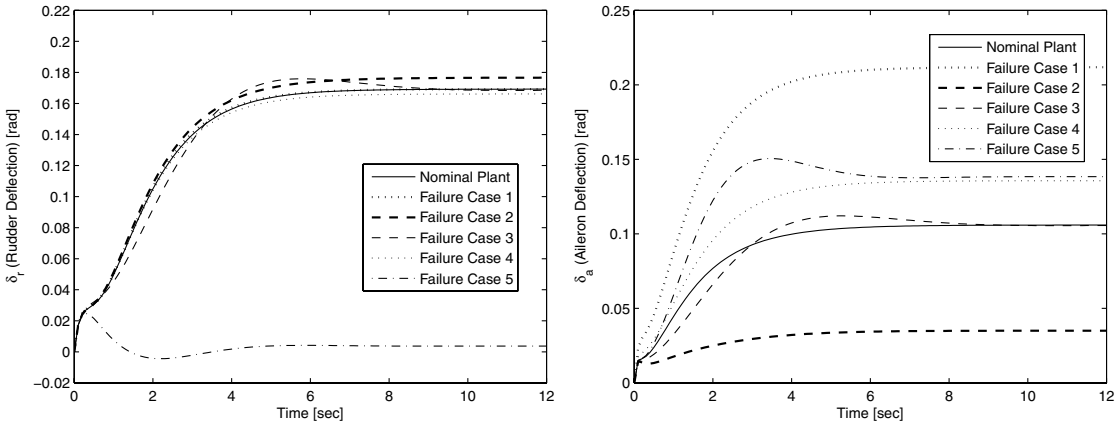

a) Rudder **b) Aileron**

Fig. 10 F4E control inputs to tracking commands.

V. Conclusions

In this paper, a decomposition approach based on a multidisciplinary design optimization formulation is proposed to numerically solve the problem of simultaneous stabilization of plants using state-feedback control. The algorithm leads to feasible solutions of the simultaneous optimal control law problem whenever such a controller exists. A top-level coordination assures that a unique state-feedback control is achieved while minimizing each plant's performance measure. At the same time, the stability of each individual plant is assured while meeting additional plant-response requirements. Results from the test cases demonstrate the ability of the algorithm to find a feasible stabilizing controller that can be implemented in an operational environment. Because only a single controller gain is needed to stabilize the aircraft at multiple flight conditions, it could potentially reduce the system complexity and improve reliability of the control system. Furthermore, the strategy can provide a feasible and robust alternative for passive fault-tolerant control.

References

[1] Saeks, R., and Murray, J., "Fractional Representation Algebraic Geometry and The Simultaneous Stabilization Problem," *IEEE Transactions on Automatic Control*, Vol. 27, No. 4, 1982, pp. 895–903. doi:10.1109/TAC.1982.1103005

[2] Birdwell, J., Castanon, D., and Athans, M., "On Reliable Control System Designs with and Without Feedback Reconfigurations," *IEEE Conference on Decision and Control*, Inst. of Electrical and Electronics Engineers, Piscataway, NJ, 1979, pp. 419–426.

[3] Vidyasagar, M., and Viswanadham, N., "Algebraic Design Techniques for Reliable Stabilization," *IEEE Transactions on Automatic Control*, Vol. 27, No. 5, 1982, pp. 1085–1095. doi:10.1109/TAC.1982.1103086

[4] Blondel, V., and Gevers, M., "Simultaneous Stabilizability of Three Linear Systems is Rationally Undecidable," *Mathematics of Control, Signals, and Systems*, Vol. 6, No. 2, 1993, pp. 135–145. doi:10.1007/BF01211744

[5] Blondel, V., and Tsitsiklis, J., "A Survey of Computational Complexity Results in Systems and Control," *Automatica*, Vol. 36, No. 9, 2000, pp. 1249–1274. doi:10.1016/S0005-1098(00)00050-9

[6] Toker, O., and Ozbay, H., "On the NP-Hardness of Solving Bilinear Matrix Inequalities and Simultaneous Stabilization with Static Output Feedback," *Proceedings of the 1995 American Control Conference*, American Automatic Control Council , Evanston, IL, 1995, pp. 2525–2526.

[7] Emre, E., "Simultaneous Stabilization with Fixed Closed-Loop Characteristic Polynomial," *IEEE Transactions on Automatic Control*, Vol. 28, No. 1, Jan. 1983, pp. 103–104. doi:10.1109/TAC.1983.1103146

[8] Barmish, B., and Wei, K., "Simultaneous Stabilizability of Single-Input Single-Output Systems," *7th International Symposium on Mathematical Theory of Networks and Systems* [CD-ROM], 1985.

[9] Henrion, D., Sebek, M., and Kucera, V., "An Algorithm for Static Output Feedback Simultaneous Stabilization of Scalar Plants," *IFAC World Congress on Automatic Control* [CD-ROM]; also Laboratoire d'Analyse et d'Architectures des Systèmes and Centre National de la Recherche Scientifique, Research Rept. 01262, Mar. 2001.

[10] Schmitendorf, W., and Hollot, C., "Simultaneous Stabilization via Linear State Feedback Control," *IEEE Transactions on Automatic Control*, Vol. 34, No. 9, 1989, pp. 1001–1005. doi:10.1109/9.35818

[11] Chow, J., "Pole-Placement Design Approach for Systems with Multiple Operating Conditions," *IEEE Transactions on Automatic Control*, Vol. 35, Mar. 1990, pp. 278–288. doi:10.1109/9.50338

[12] Chen, H., Chow, J., Kale, M., and Minto, K., "Simultaneous Stabilization Using Stable System Inversion," *Automatica*, Vol. 31, No. 4, 1995, pp. 531–542. doi:10.1016/0005-1098(95)98482-L

[13] Wu, D., Gao, W., and Chen, M., "Algorithm for Simultaneous Stabilization of Single-Input Systems via Dynamic Feedback," *International Journal of Control*, Vol. 51, No. 3, 1990, pp. 631–642. doi:10.1080/00207179008934089

[14] Howitt, G., and Luus, R., "Simultaneous Stabilization of Linear Single Input Systems By Linear State Feedback Control," *International Journal of Control*, Vol. 54, No. 4, 1991, pp. 1015–1030. doi:10.1080/00207179108934197

[15] Geromel, J., Peres, P., and Souza, S., "On a Convex Parameter Space Method for Linear Control Design of Uncertain Systems," *SIAM Journal on Control and Optimization*, Vol. 29, No. 2, 1991, pp. 381–402. doi:10.1137/0329021

[16] Howitt, G., and Luus, R., "Control of a Collection of Linear Systems by Linear State Feedback Control," *International Journal of Control*, Vol. 58, No. 1, 1993, pp. 79–96. doi:10.1080/00207179308922992

[17] Paskota, M., Sreeram, V., Teo, K., and Mees, A., "Optimal Simultaneous Stabilization of Linear Single-Input Systems via Linear State Feedback Control," *International Journal of Control*, Vol. 60, No. 4, 1994, pp. 483–498. doi:10.1080/00207179408921477

[18] Luke, R., Dorato, P., and Abdallah, C., "Linear-Quadratic Simultaneous Performance Design," *Proceedings of the 1997 American Control Conference*, American Automatic Control Council , Evanston, IL, 1997, pp. 3602–3605.

[19] Lam, J., and Cao, Y., "Simultaneous Linear-Quadratic Optimal Control Design via Static Output Feedback," *International Journal of Robust and Nonlinear Control*, Vol. 9, No. 9, 1999, pp. 551–558. doi:10.1002/(SICI)1099-1239(19990730)9:9<551::AID-RNC420>3.0.CO;2-9

[20] Balakrishnan, V., and Vandenberghe, L., "Connections Between Duality in Control Theory and Convex Optimization," *Proceedings of the 1995 American Control Conference*, American Automatic Control Council , Evanston, IL, 1995, pp. 4030–4034.

[21] Dorato, P., Abdallah, C. T., and Cerone, V., *Linear Quadratic Control: An Introduction*, Prentice–Hall, Englewoods Cliffs, NJ, 1995.

[22] Nocedal, J., and Wright, S., *Numerical Optimization*, 1st ed., Series in Operational Research, Springer–Verlag, New York, 1999.

[23] Ackermann, J., *Longitudinal Control of Fighter Aircraft F4E with Additional Canards, in a Collection of Plant Models and Design Specifications for Robust Control*, DFVLR Press, Oberpfaffenhoffen, Germany, 1982.

[24] Kharitonov, V. L., "Asymptotic Stability of an Equilibrium Position of a Family of Systems of Linear Differential Equations," *Differentsialnye Uravneniya*, Vol. 14, 1978, pp. 2086–2088.

[25] Bryson, A., and Ho, Y., *Applied Optimal Control: Optimization, Estimation, and Control*, Hemisphere, New York, 1975.

[26] Liu, H., and Berndt, H., "Interactive Design and Simulation Platform for Flight Vehicle Systems Development," *Journal of Aerospace Computing, Information, and Communication*, Vol. 3, No. 11, Nov. 2006, pp. 550–561.

[27] Huang, C., and Stengel, R., "Restructurable Control Using Proportional-Integral Implicit Model Following," *Journal of Guidance, Control, and Dynamics*, Vol. 13, No. 2, Mar.–Apr. 1990, pp. 303–309.